1,3-Dioxane-Linked Bacterial Topoisomerase Inhibitors with Enhanced Antibacterial Activity and Reduced hERG Inhibition

Linsen Li,[†] Antony A. Okumu,[†] Sheri Nolan,[‡] Anthony English,[§] Sandip Vibhute,[†] Yanran Lu,[†] Katherine Hervert-Thomas,[‖] Justin T. Seffernick,[⊥] Lovette Azap,[†] Serena L. Cole,[¶] D. Shinabarger,[¶] Laura M. Koeth,[□] Steffen Lindert,[⊥] Jack C. Yalowich,[§] Daniel J. Wozniak,[‡,■] and Mark J. Mitton-Fry*[,†]

[†]Division of Medicinal Chemistry and Pharmacognosy, The Ohio State University, 500 West 12th Avenue, Columbus, Ohio 43210, United States

[‡]Microbial Infection and Immunity, The Ohio State University, 460 West 12th Avenue, Columbus, Ohio 43210, United States

[§]Division of Pharmacology, The Ohio State University, 500 West 12th Avenue, Columbus, Ohio 43210, United States

[‖]Department of Chemistry, Ohio Wesleyan University, 61 South Sandusky Street, Delaware, Ohio 43015, United States

[⊥]Department of Chemistry and Biochemistry, The Ohio State University, 100 West 18th Avenue, Columbus, Ohio 43210, United States

[¶]Micromyx, 4717 Campus Drive, Kalamazoo, Michigan 49008, United States

[□]Laboratory Specialists, Inc., 26214 Center Ridge Road, Westlake, Ohio 44145, United States

[■]Department of Microbiology, The Ohio State University, 484 West 12th Avenue, Columbus, Ohio 43210, United States

S Supporting Information
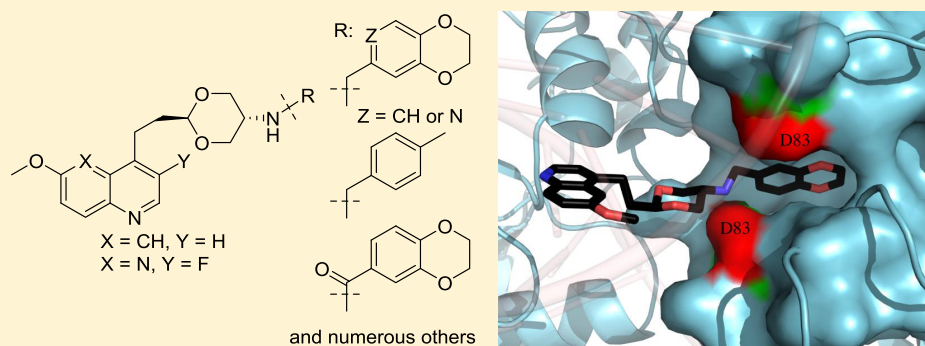
ABSTRACT: The development of new therapies to treat methicillin-resistant *Staphylococcus aureus* (MRSA) is needed to counteract the significant threat that MRSA presents to human health. Novel inhibitors of DNA gyrase and topoisomerase IV (TopoIV) constitute one highly promising approach, but continued optimization is required to realize the full potential of this class of antibiotics. Herein, we report further studies on a series of dioxane-linked derivatives, demonstrating improved antistaphylococcal activity and reduced hERG inhibition. A subseries of analogues also possesses enhanced inhibition of the secondary target, TopoIV.

KEYWORDS: methicillin-resistant *Staphylococcus aureus*, novel bacterial-topoisomerase inhibitors, gyrase

Infections caused by multidrug-resistant bacteria pose a significant challenge to the practice of modern medicine.[1] MRSA infection occurs in a wide variety of clinical settings, including bacteremia, endocarditis, pneumonia, and skin infection as well as in individuals living with cystic fibrosis.[2,3] The number of deaths attributed to MRSA infection is particularly high as compared with other multidrug-resistant pathogens.[4] Although recent years have seen a number of approvals for new antibiotics with potent anti-MRSA activity, these compounds are derived from existing classes of antibiotics,[5−9] and resistance has already been observed in

some cases.[10] Consequently, new antibiotic classes are urgently needed. Novel bacterial topoisomerase inhibitors (NBTIs),[11,12] which inhibit the same targets as the fluoroquinolones but avoid cross-resistance,[13] are one particularly promising option. The NBTI class possesses potent antistaphylococcal activity. A recent elegant study of the pharmacology of gepotidacin,[14] an NBTI that has advanced to Phase 2 clinical trials,[15,16] demonstrated that it
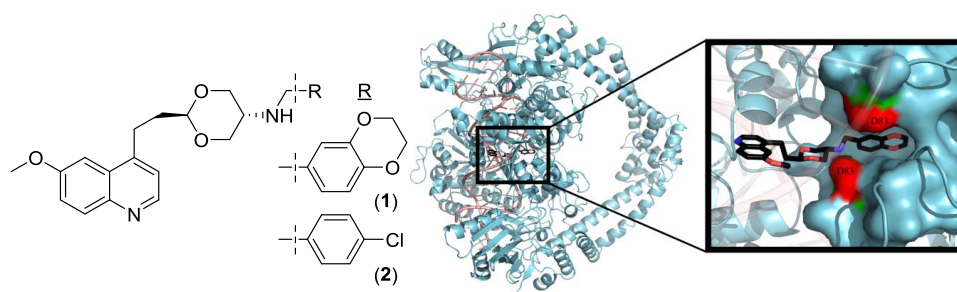
Figure 1. Previously reported dioxane-linked NBTIs[25] (left) and proposed binding mode of compound **1** to *S. aureus* DNA gyrase (right, DNA rendered semitransparent for clarity).

potently inhibits DNA gyrase in *Staphylococcus aureus* through the induction of stable single-stranded breaks in DNA. Nevertheless, the translational development of many of these agents has been hampered by cardiovascular-safety concerns[11,17−20] (primarily hERG inhibition) and by resistance observed via single amino acid substitutions in DNA gyrase.[11,21−24] Consequently, additional research efforts directed at optimization of this promising novel antibiotic class are highly warranted.

We recently disclosed a series of 5-amino-1,3-dioxane-linked NBTIs with potent antistaphylococcal activity.[25] In line with previously reported crystallographic studies,[13,14,26] we propose that compounds such as **1** form a ternary complex with DNA and DNA gyrase (Figure 1), with the quinoline moiety binding to DNA and the dihydrobenzodioxine moiety filling a small hydrophobic pocket in DNA gyrase. The dioxane serves to link these two motifs and acts as a handle for the modulation of physicochemical properties such as lipophilicity and basicity.[25] The majority of NBTIs employ a fused, bicyclic enzyme-binding moiety,[27] as seen in **1**. Exceptions include certain antitubercular NBTIs[28−31] as well as antistaphylococcal NBTIs with carboxypiperidine linkers, for example, NXL-101[21] and the previously reported arylcyclobutane derivatives.[22,32] In this new series of dioxane-linked NBTIs, fused, bicyclic enzyme-binding moieties such as that of **1** were also advantageous. Intriguingly, however, monocyclic 4-chlorophenyl derivatives (such as in **2**) also proved surprisingly potent against *S. aureus*. Additional advantages to dioxane-linked NBTIs were observed when comparing hERG inhibition versus a series of matched-pair[33] controls with either piperidine or cyclohexyl linkers, consistent with the design hypothesis.[25] The current work focuses on efforts to establish a broader understanding of structure−activity relationships of the enzyme-binding motif, to enhance the whole-cell antibacterial activity further, improve the inhibition of the secondary enzyme target (TopoIV), and reduce hERG inhibition further.

RESULTS AND DISCUSSION

Encouraged by our previous results, a diverse set of compounds with both monocyclic and fused bicyclic enzyme-binding moieties was synthesized using the previously described route.[25] A 6-methoxyquinoline DNA-binding motif was employed in the initial survey because of ease of synthesis. Minimum inhibitory concentrations (MICs) were determined according to Clinical and Laboratory Standards Institute (CLSI) guidelines[34] using *S. aureus* ATCC 29213 as a reference strain. Compounds with MICs ≤64 μg/mL were also assayed using a ciprofloxacin-resistant USA 300 strain of MRSA, as we described previously.[25] Given the objective to

enhance dual-targeting activity so as to reduce the rate of resistance emergence, biochemical assays were also employed on a subset of compounds (minimally those with *S. aureus* ATCC 29213 MICs ≤2 μg/mL) to measure inhibition of both DNA gyrase and TopoIV.

On the basis of 4-chlorophenyl derivative **2**, a variety of analogues bearing a 4-substituted phenyl ring were prepared and assayed (Table 1). Analogues possessing methyl (**3**), trifluoromethyl (**4**), methoxy (**5**), and trifluoromethoxy (**6**) groups possessed *S. aureus* MICs ranging from 1 to 4 μg/mL, a dramatic improvement from that of the unsubstituted analogue (**7**, >64 μg/mL[25]). The smaller fluoro (**8**) and more polar cyano (**9**) analogues lacked activity, whereas the large and lipophilic *tert*-butyl moiety (**10**) was tolerated. Additionally, none of these compounds tested for TopoIV activity (**2−5**, **9**, and **10**) potently inhibited this enzyme (IC$_{50}$ values >100 μM). The more polar methylpyridine analogue, **11**, was moderately less potent than the analogous phenyl compound, **3**. Cyclohexyl analogue **12** had modest activity that was somewhat improved by incorporation of a 4-methyl substituent, as in **13** (MICs of 8 and 2 μg/mL, respectively).

Bax and co-workers elucidated the binding mode of the NBTI class of antibiotics by determination of the X-ray crystal structure of GSK299423 in a ternary complex with DNA and DNA gyrase.[13] Their structure suggested the presence of an unusual hydrogen bond between the methylene of the oxathiolopyridine ring and the backbone carbonyl of A68 in DNA gyrase. We hypothesized that a similar nontraditional hydrogen bond might also be achieved by a difluoromethoxy (**14**, Figure 2) or difluoromethyl (**15**) substituent. Unfortunately, although both compounds showed MICs ≤8 μg/mL, neither proved to be an improvement over the nonfluorinated (**5** and **3**) or fully fluorinated (**6** and **4**) parent molecules.

In line with our prior experience,[25] 3-substituted phenyl analogues (**16−19**) displayed only very modest MICs (16−64 μg/mL), and the 2-substituted derivatives (**20−22**) were wholly devoid of activity (Table 1). A variety of dihalogenated compounds were also synthesized, but only the 4-chloro-3-fluoro derivative (**23**, 2 μg/mL) and the isomeric 3-chloro-4-fluoro analogue (**24**, 8 μg/mL) showed single-digit MICs (Table 1).

Our previous report[25] employed several prototypical fused, bicyclic enzyme-binding motifs, which universally delivered potent MICs, so additional analogues in this subseries were also synthesized and assayed (Table 1). Ring contraction of **1**, as in benzodioxole[35] **26**, resulted in somewhat poorer MICs. Difluorination, as in **27**, slightly improved activity. Unfortunately, neither of these analogues potently inhibited TopoIV. The fully unsaturated lipophilic 2-naphthyl analogue, **28**, was

Table 1. Antibacterial and Biochemical Activities of NBTIs with 6-Methoxyquinoline Moieties
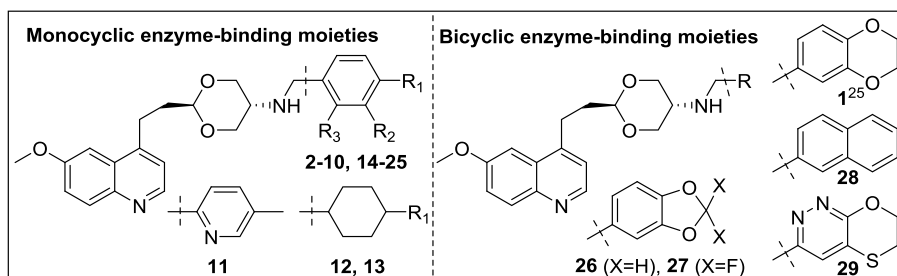

compd (R_1, R_2, R_3)	S. aureus (MSSA) ATCC 29213 MIC (μg/mL)[a,b]	S. aureus (MRSA) USA 300 MIC (μg/mL)[a,b]	S. aureus DNA gyrase IC$_{50}$ (μM)[c]	S. aureus TopoIV IC$_{50}$ (μM)[d]
1[25] (see above)	0.25−1	0.5	0.10	14
2[25] (Cl, H, H)	1	4	1.2	>100
3 (Me, H, H)	1	1	0.22	>100
4 (CF$_3$, H, H)	1	2	0.3	~100
5 (OMe, H, H)	4	8	1.5	>100
6 (OCF$_3$, H, H)	2	4	2.1	18[e]
7[25] (H, H, H)	>64	NT	NT	NT
8 (F, H, H)	>64	NT	NT	NT
9 (CN, H, H)	>64	NT	13	>100
10 (t-Bu, H, H)	2	4	0.63	>100
11 (see above)	4−8	16	NT	NT
12 (R_1 = H)	8	8	NT	NT
13 (R_1 = Me, mix of cis and trans)	2	2	0.77	67[f]
14 (OCF$_2$H, H, H)	4−8	8	NT	NT
15 (CHF$_2$, H, H)	2	4	0.36	>100
16 (H, CN, H)	64	128	NT	NT
17 (H, OMe, H)	4−16	32	NT	NT
18 (H, Me, H)	16	32	NT	NT
19 (H, F, H)	32	>32	NT	NT
20 (H, H, OMe)	>64	NT	NT	NT
21 (H, H, Me)	>64	NT	NT	NT
22 (H, H, F)	>64	NT	NT	NT
23 (Cl, F, H)	2	1	0.95	>100
24 (F, Cl, H)	8	8	2.1	>100
25 (F, F, H)	64	64	NT	NT
26 (see above)	2	4	0.17	74
27 (see above)	1	2	0.52	>100
28 (see above)	1	2	0.69	6.3[e]
29 (see above)	1	2	0.81	13[e]
30 (Figure 3)	>8	>8	7.7	>100[f]
31 (Figure 3)	0.5	1	1.1	>200[e]
ciprofloxacin	0.125−0.5	16−32	13.3	4.0
vancomycin	NT	0.5−2	NT	NT

[a]Assays were conducted according to CLSI broth-microdilution guidelines[34] (n = 3, minimum). [b]Ranges of observed values provided where appropriate. [c]Determined at Inspiralis (Norwich, U.K.; n = 2, minimum). [d]Method A (see the Experimental Section). Determined at Inspiralis (Norwich, U.K.; n = 2, minimum). [e]Method B (see the Experimental Section, n = 2). [f]Method B (n = 1).

similar in antistaphylococcal potency and inhibited TopoIV with an IC$_{50}$ of 6.3 μM. Compound 29, bearing the oxathiinopyridazine moiety,[23] was similar to compound 1 in terms of both antistaphylococcal activity and TopoIV inhibition.

Inspection of several ternary crystal structures of DNA, DNA gyrase, and NBTIs reported by GSK[13,36,37] (PDB codes 2XCS, 4BUL, and 5IWI) revealed two alternate NBTI binding poses as a result of the symmetric nature of the hydrophobic pocket formed from the two GyrA domains. Superposition of these ligands (silver and black in Figure 3) suggested that the entrance to the hydrophobic pocket may be sufficiently wide to

accommodate moieties such as the 1-naphthyl group of 30. Unfortunately, the compound was a poor inhibitor of gyrase (IC$_{50}$ of 7.7 μM) and failed to demonstrate antibacterial activity at concentrations up to 8 μg/mL (Table 1). The SAR of the monocyclic derivatives (vide supra) suggested, however, that gyrase inhibition and antibacterial activity may require a substituent that extends further into the hydrophobic pocket. Consequently, acenaphthylene derivative 31 was synthesized and evaluated. Compound 31 demonstrated gyrase inhibition (IC$_{50}$ of 1.1 μM) and antibacterial activity (S. aureus ATCC 29213 MIC = 0.5 μg/mL) similar to 28, suggesting that the lack of activity in 30 originated not from its width but from the
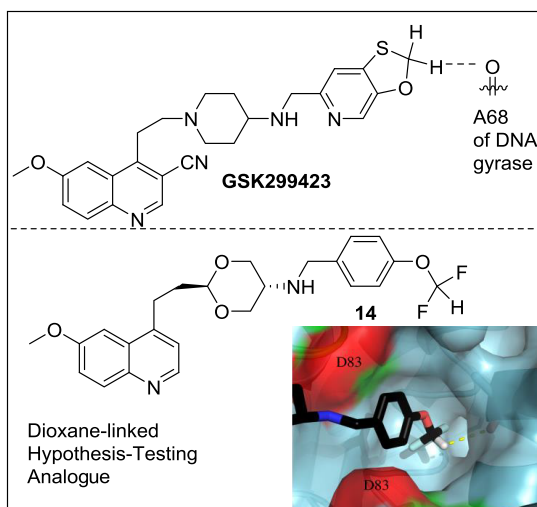
Figure 2. Nontraditional hydrogen bonding observed for GSK299423[13] and proposed for novel analogue **14**.

absence of binding deeper in the enzyme pocket. Unfortunately, **31** showed no inhibition of TopoIV (Table 1). That observation, coupled with its extreme lipophilicity (cLogP = 5.7) led to deprioritization of additional efforts on this analogue.

Having established a general understanding of structure–activity relationships for the enzyme-binding moiety of these dioxane-linked NBTIs, we sought to enhance the antibacterial activity through incorporation of a 7-fluoro-2-methoxy-1,5-naphthyridine DNA-binding moiety.[20,23,26,32,38,39] Compounds were synthesized via a modification of our previously published route (Scheme 1).[25] Briefly, naphthyridinol **32** was brominated with PBr$_3$ to afford the bromonaphthyridine derivative **33** in 90% yield. Hydroboration of alkene **34** with 9-BBN followed by Suzuki coupling with **33** afforded intermediate **35** in 58% yield. Deprotection of the phthalimide was accomplished using ethanolamine in refluxing ethyl acetate as previously reported[25,40] to afford the primary amine, **36**, as a key intermediate. Final analogues (**37–42**) were synthesized by reductive amination under our previously described conditions.[25]

As expected, compounds **37–40** bearing previously demonstrated enzyme-binding moieties,[25] displayed very potent MICs ($\leq$0.25 μg/mL) against both the ATCC *S. aureus* and MRSA strains, as did the oxathiinopyridazine[23,39] analogue, **41** (Table 2). Naphthyridine analogues with suboptimal enzyme-binding moieties, such as the 3,4-

difluorophenyl derivative, **42**, displayed markedly improved MICs as compared with that of the 6-methoxyquinoline analogue, **25** (2 vs 64 μg/mL, respectively), although the activity was still modest in comparison with those of **37–41**. Although we did not prepare a comprehensive set of matched-pair analogues, we observed that the SAR in the naphthyridine series largely mirrored that of the quinoline series, with consistently enhanced whole-cell activity.

Inhibition of DNA gyrase and TopoIV was also generally improved for this series of naphthyridine derivatives (Table 2). Particularly exciting was compound **37**, with a TopoIV IC$_{50}$ of 0.98 μM, representing a significant step forward in the effort to discover potent dual-target inhibitors. Compound **38** showed less-potent TopoIV inhibition (IC$_{50}$ = 51 μM) using the standard conditions (Method A, see the Experimental Section for details), but additional experiments suggested that solubility issues may have confounded that assessment. Consequently, further studies were conducted in-house for compound **38** using a slightly modified method (Method B) with careful monitoring for solubility, revealing an IC$_{50}$ of 2.4 μM. Compound **37** was used to validate the in-house assay; the IC$_{50}$ values determined by both methods were highly consistent. Compounds **37–41** showed potent TopoIV inhibition similar to that of **37** using Method B.

In order to better understand the ability of compound **37** and related analogues to inhibit TopoIV, we constructed a computational homology model and examined a potential binding pose for **37** (see the Experimental Section for additional details). As shown in Figure 4, the overall binding mode is similar to that proposed for compound **1** binding to DNA gyrase (Figure 1). Efforts toward further refinement of this model, along with its use in the prospective design of superior TopoIV inhibitors, is ongoing.

As a result of their distinctive binding mode, NBTIs are expected to maintain activity in the presence of mutations that confer resistance to fluoroquinolones.[13] The S84L amino acid substitution in gyrase is one prototypical example.[21,23,39] We tested the inhibitory activities of three representative naphthyridine analogues (**37**, **38**, and **41**) and ciprofloxacin against *S. aureus* gyrase with the S84L substitution (Table 3; for ease of comparison, the IC$_{50}$ values against the wild-type gyrase from Table 2 are duplicated here). Compounds **37** and **41** showed equipotent inhibition of the S84L gyrase, whereas **38** showed slightly diminished activity (4-fold loss). Ciprofloxacin, in contrast, showed ~15-fold loss of activity. Moreover, *gyrA* sequencing of the USA 300 MRSA isolate used in the current work demonstrated that this strain contains the S84L substitution (see the Experimental Section). The
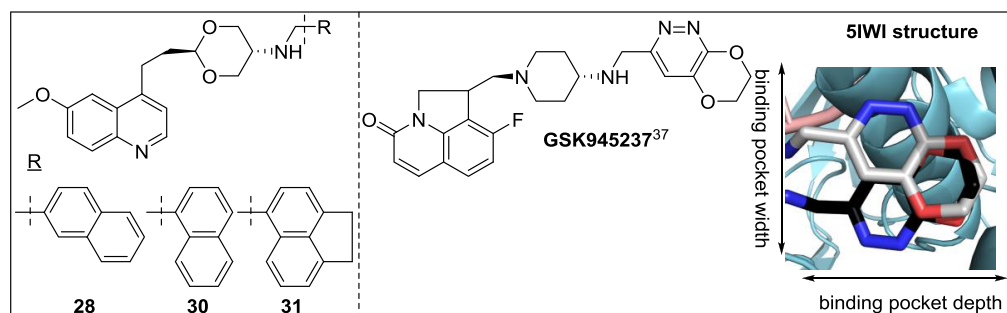
Figure 3. Design of "wider" NBTIs informed by published crystal structures.
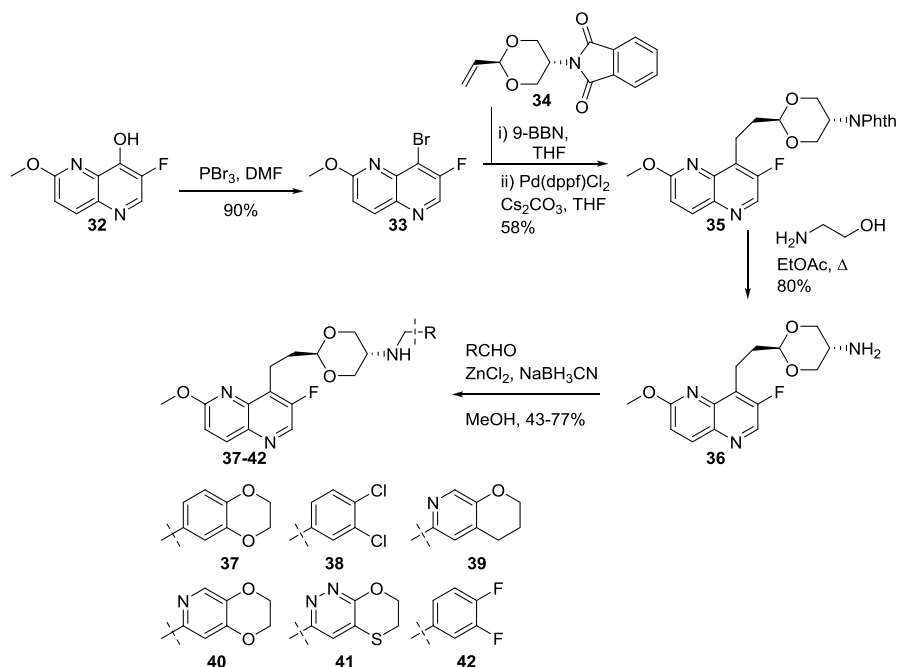
Scheme 1. Synthesis of Compounds 37−42

Table 2. Antibacterial and Biochemical Activities of NBTIs with 7-Fluoro-2-methoxynaphthyridine Moieties

compd	$S.$ $aureus$ (MSSA) ATCC 29213 MIC (μg/mL)[a,b]	$S.$ $aureus$ (MRSA) USA 300 MIC (μg/mL)[a,b]	$S.$ $aureus$ DNA gyrase IC$_{50}$ (μM)[c]	$S.$ $aureus$ TopoIV IC$_{50}$ (μM)[d]
37	≤0.25, 0.25	0.125	0.03	0.98, 1.0[e]
38	0.25	0.125	0.04	51, 2.4[e]
39	≤0.25, 0.125	0.25	0.16	5.3, 0.71[e]
40	0.125	0.125−0.25	0.42	18, 4.3[e]
41	0.25	0.25	0.07	0.76[f]
42	2	4	4.43	>100
1[25]	0.25−1	0.5	0.10	14
ciprofloxacin	0.125−0.5	16−32	13.3	4.0, 8.6[f]
vancomycin	NT	0.5−2	NT	NT

[a]Assays were conducted according to CLSI broth-microdilution guidelines[34] (n = 3, minimum). [b]Ranges of observed values provided where appropriate. [c]Determined at Inspiralis (Norwich, U.K.; n = 2, minimum). [d]Method A (see the Experimental Section). Determined at Inspiralis (Norwich, U.K.; n = 2, minimum). [e]Method B (see the Experimental Section, n = 2, minimum). [f]Method B (n = 1).
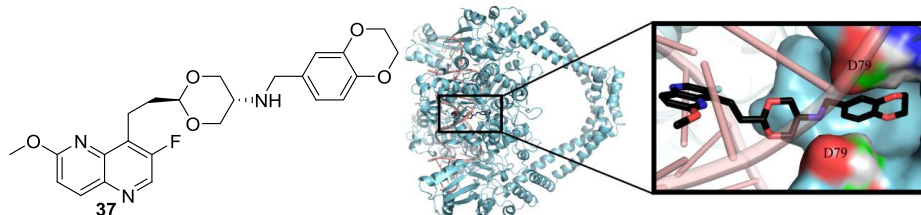

Figure 4. Structure and binding mode of compound 37 with TopoIV, as predicted using computational homology modeling (DNA rendered semitransparent for clarity).

Table 3. Inhibition of Wild-Type and Fluoroquinolone-Resistant (S84L) DNA Gyrase

compd	$S.$ $aureus$ wild-type DNA gyrase IC$_{50}$ (μM)[a]	$S.$ $aureus$ S84L DNA gyrase IC$_{50}$ (μM)[a]
37	0.03	0.018
38	0.04	0.16
41	0.07	0.065
ciprofloxacin	13.3	209.9

[a]Determined at Inspiralis (Norwich, U.K.; n = 2, minimum).

consistent MICs for our NBTIs between the $S.$ $aureus$ ATCC 29213 and USA 300 strains are further evidence of the lack of cross-resistance.

Representative potent fluoronaphthyridine-series analogues 37−40 were also assayed in spontaneous frequency-of-resistance (FoR) studies using $S.$ $aureus$ ATCC 29213 as the test organism and ciprofloxacin as a control. These compounds displayed especially potent MICs by the agar-dilution method (Table 4); FoR values were determined at 4× and 8× multiples of the agar MIC. As shown, FoR values in the 10^{-7}

Table 4. Spontaneous Frequency of Resistance[a]

| compd | S. aureus ATCC 29213 MIC[b] (μg/mL) | spontaneous-mutation frequency | |
		4× MIC	8× MIC
37	0.015	1.53×10^{-7}	4.5×10^{-8}
38	0.015	2.31×10^{-7}	1.62×10^{-7}
39	0.015	6.75×10^{-7}	1.67×10^{-7}
40	0.03	2.26×10^{-7}	1.08×10^{-7}
ciprofloxacin	0.25	1.15×10^{-8}	$<7.69 \times 10^{-10}$

[a]See the Experimental Section for full details. [b]Assays were conducted according to CLSI agar-dilution guidelines[34,42] ($n = 2$).

range were observed across the series, with only modest improvements at the 8× concentrations. The observed frequencies are similar to those reported for other NBTIs against this strain: ACT-387042[39] (3.0×10^{-8} at 4×) and AM-8722[41] (6.7×10^{-7} at 4×). We conclude that further optimization of TopoIV-inhibitory potency is needed to afford substantially reduced FoR values.

The potent antistaphylococcal activity observed for these dioxane-linked NBTIs prompted an assessment of the potential for broader-spectrum activity as well as a more thorough test of the activity against fluoroquinolone-resistant S. aureus. Table 5 shows MICs against a variety of both Gram-positive and Gram-negative pathogens for 37, the aza-analogue (40), and the oxathiinopyridazine (41). All three compounds showed potent whole-cell activity for Gram-positive pathogens, including fluoroquinolone-resistant MRSA, vancomycin-resistant Enterococcus faecium (VRE), and penicillin-resistant Streptococcus pneumoniae. Compound 41 demonstrated a potent MIC_{90} value of 0.12 μg/mL when tested against 11 strains of fluoroquinolone-resistant S. aureus (as compared with ciprofloxacin, which had an MIC_{90} of 32 μg/mL). Additionally, anti-Gram-negative activity was also seen for Pseudomonas aeruginosa and especially for compound 41 against Acinetobacter baumannii. These results raise the exciting prospect that further structural optimization might yield new leads for treating these critically important pathogens, as has been reported for other series of NBTIs.[43,44]

As an initial assessment of compound safety, we measured hERG inhibition (vide infra) and assayed for potential mammalian cytotoxicity with human leukemia K562 cells as previously reported[25] (Table 6). By comparing MIC values from Tables 1 and 2 with K562 growth-inhibition IC_{50} values (Table 6), we calculated a preliminary selectivity index (after converting to the same concentration units). Naphthyridine analogues 38−40 displayed a substantial selectivity index (50- to 100-fold), whereas 37 and 41 were more modest (7- and 15-fold, respectively). There are limitations to this type of preliminary analysis because of differences between the assays, such as the presence of a small amount of serum and direct cell counting in the K562 assay. Nevertheless, the comparison demonstrates the promise of selective toxicity toward bacterial cells. Furthermore, compounds were also evaluated using K/VP.5 cells, an etoposide-resistant subclone with reduced expression of human topoisomerase IIα.[45,46] Similar inhibitory activity was seen in both K562 and K/VP.5 cells, suggesting a lack of inhibition of the orthologous human target. This finding was further supported by biochemical assays using the isolated human topoisomerase IIα. No compounds displayed >50% inhibition of decatenation at 100 μM concentration. Given the lack of significant human topoisomerase IIα inhibition at this high concentration, IC_{50} values against the human target were not determined.

Cardiovascular safety, as manifested by hERG inhibition, has presented a significant obstacle to the successful development of the NBTI class of antibiotics.[11,17−20,43,44] We designed dioxane-linked NBTIs with the hypothesis that the two electronegative oxygen atoms would reduce nitrogen basicity,[25,47] and our initial studies demonstrated reduced hERG inhibition by matched-pair analysis with other linkers.[25] Table 6 provides hERG-inhibition data for selected compounds from the current study. Within the quinoline series, the lipophilic 4-substituted phenyl analogues were potent hERG inhibitors, with IC_{50} values of ≤5 μM across the series. Direct comparison of various naphthyridine derivatives (37−40) with the previously reported[25] quinoline analogues showed only minor differences (<2-fold change in either direction), and the oxathiino analogues 29 (quinoline) and 41 (naphthyr-

Table 5. Broad-Spectrum Antibacterial Activity of Select NBTIs

| strain | MIC (μg/mL)[a] | | | |
	compd 37	compd 40	compd 41	ciprofloxacin
S. aureus ATCC 29213 ($n = 3$)	≤0.06[b]	≤0.06[b]	≤0.06[b]	0.25
MRSA DRL-3161	≤0.06	≤0.06	≤0.06	>64
Streptococcus pyogenes LSI-1235	≤0.06	≤0.06	≤0.06	0.25
Streptococcus pneumoniae LSI-4234[c]	0.25	0.5	0.25	2
Streptococcus pneumoniae LSI-4246[d]	≤0.06	≤0.06	≤0.06	0.5
Enterococcus faecium DRL-4193[e]	0.12[f]	0.5	0.25[g]	0.25
Enterococcus faecium LSI-3340[h]	0.12	0.25	0.25	16
Enterococcus faecalis ATCC 29212	0.5	1	0.5	0.5
Fluoroquinolone-resistant S. aureus (11 strains)	NT	NT	0.12 (MIC_{90})	32 (MIC_{90})
Escherichia coli ATCC 25922 ($n = 2$)	16	64	32	≤0.06
Pseudomonas aeruginosa LSI-2946	4	8	8	0.5
Acinetobacter baumannii LSI-2957	2	1	≤0.06	0.25
Klebsiella pneumoniae LSI-2999	>64	>64	>64	0.25
Enterobacter cloacae LSI-2943	32	>64	>64	≤0.06

[a]Determined according to CLSI broth-microdilution guidelines.[34] [b]Very small pinpoint growth up to 4 μg/mL; no viable growth from pinpoint wells. [c]Penicillin-susceptible. [d]Penicillin-resistant. [e]Vancomycin-susceptible. [f]Trailing observed; no viable growth within trailing wells. [g]Pinpoint growth through 64 μg/mL. [h]Vancomycin-resistant.

Table 6. In Vitro Safety Assessment of Selected NBTIs

compd	hERG IC$_{50}$ (μM)[a]	K562 IC$_{50}$ (μM)	K/VP.5 IC$_{50}$ (μM)	hTopoII (% inhibition at 100 μM)[b]
3	4.4	17	25	11.5
4	3.4	8.9	12	1.8
6	3.2	13	14	3.8
10	4.7	7.6	6.3	−2.1
26	8.6	25	26	14.4
27	5.0	14	14	0.9
29	12	28	20	−3.1
37	8.0	3.4	3.1	45.0
38	7.9	29	25	5.1
39	9.3	53	46	20.2
40	15	69	62	30.4
41	13	7.5	7.6	3.6
cisapride[c]	0.012−0.021	NT	NT	NT
etoposide	NT	0.3	5.1	63.9 (n = 6)
ciprofloxacin	NT	NT	NT	12.3 (n = 6)

[a]Determined using IonWorks Barracuda (Charles River, Cleveland, OH). [b]Percent inhibition calculated as 100 minus percent activity (Inspiralis, Ltd., Norwich, U.K.). [c]Cisapride serves as the positive control for the hERG study.

Table 7. NBTIs Designed for Reduced hERG Inhibition with Associated Assay Data
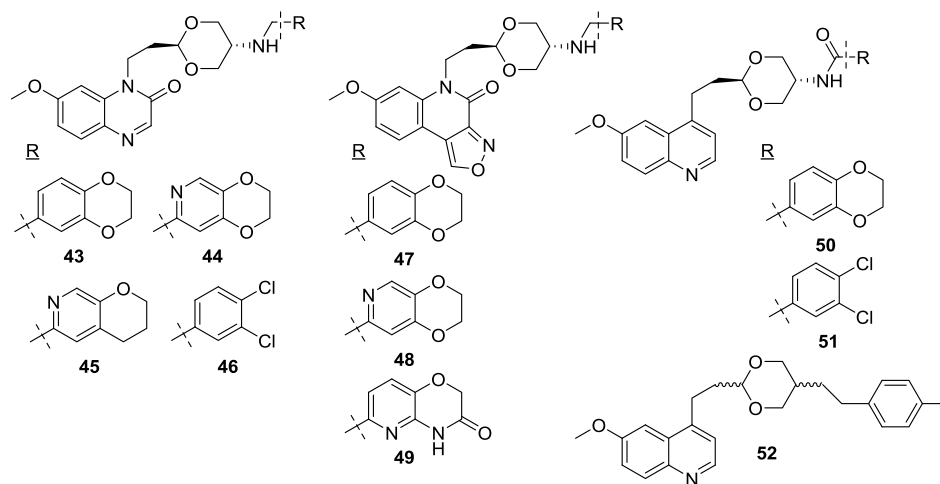
compd	S. aureus (MSSA) ATCC 29213 MIC (μg/mL)[a,b]	S. aureus (MRSA) USA 300 MIC (μg/mL)[a,b]	hERG IC$_{50}$ (μM)[c]	S. aureus DNA gyrase IC$_{50}$ (μM)[d]	S. aureus TopoIV IC$_{50}$ (μM)[e]
43	4−32	32	6.6	2.0	>100[f]
44	8−32	32	NT	NT	NT
45	8−16	32	NT	NT	NT
46	4−16	>64	NT	NT	NT
47	1	1	>10	0.32	>200
48	1	2	>30	0.83	>200
49	4	2	NT	NT	NT
50	1	1	>100	3.7	>200
51	0.125	0.125	3.2	0.59	>200
52	>64	NT	NT	NT	NT
1[25]	0.25−1	0.5	5.1	0.10	14
ciprofloxacin	0.125−0.5	16−32	NT	13.3	4.0,[f] 8.6[e]
vancomycin	NT	0.5−2	NT	NT	NT
cisapride[g]	0.012−0.021	NT	NT	NT	NT

[a]Assays were conducted according to CLSI broth-microdilution guidelines[34] (n = 3, minimum). [b]Ranges of observed values provided where appropriate. [c]Determined using IonWorks Barracuda (Charles River, Cleveland, OH). [d]Determined at Inspiralis (Norwich, U.K.; n = 2, minimum). [e]Method B (see the Experimental Section, n = 1). [f]Method A (see the Experimental Section). Determined at Inspiralis (Norwich, U.K.; n = 2, minimum). [g]Cisapride serves as the positive control for the hERG study.

idine) followed the same trend. The improved antibacterial activity of the naphthyridines vis-à-vis the quinolines suggests an improved therapeutic index. For example, compound **40** is a

modestly less potent hERG inhibitor with roughly 8-fold improvement in MICs as compared with the previously reported quinoline analogue[25] (S. aureus ATCC 29213 MIC

= 0.125 vs 1−2 μg/mL and hERG IC$_{50}$ = 15 vs 9.5 μM). We targeted an hERG IC$_{50}$ of ~100 μM as being consistent with a favorable profile for a lead compound.[32,44] Thus, although the dioxane moiety presents an advantage as compared with other linkers,[25] additional improvements are clearly necessary.

Three approaches were taken to mitigate this issue: (1) use of a more polar DNA-binding moiety, (2) replacement of the amine by an amide, and (3) removal of the secondary amine. In the first instance, four N-linked quinoxalinone analogues[48] (43−46, Table 7) were synthesized (see the Supporting Information). Unfortunately, these compounds displayed inferior antibacterial activity. Compound 43 demonstrated reduced DNA-gyrase inhibition (IC$_{50}$ = 2.0 μM), no meaningful TopoIV inhibition (IC$_{50}$ > 100 μM), and no inhibition of human topoisomerase IIα (2.5% inhibition at 100 μM). Moreover, compound 43 showed an hERG IC$_{50}$ of 6.6 μM (i.e., no improvement as compared with earlier compounds). Three N-linked analogues containing the recently reported isoxazoloquinolinone DNA-binding moiety[49] (47−49) were also synthesized (see the Supporting Information). Compounds 47 and 48 had submicromolar gyrase IC$_{50}$ values and MICs of 1−2 μg/mL against S. aureus ATCC 29213 and MRSA. Limited inhibition of human topoisomerase IIα was demonstrated at 100 μM (16% for 47 and 38% for 48). Compounds 47 and 48 also afforded modestly improved hERG profiles, but solubility limitations precluded determination of IC$_{50}$ values in both cases. Additionally, compounds 47 and 48 did not inhibit TopoIV at concentrations up to 200 μM (Table 7).

Limited literature precedent supports the replacement of the NBTI secondary amine by a secondary amide.[35,50−52] Additionally, the replacement of the basic nitrogen would be expected to confer diminished hERG inhibition. Compounds 50 and 51 (Table 7) were synthesized to test this hypothesis. Both analogues, especially 51, displayed potent MICs against S. aureus ATCC 29213 and MRSA, and the enhanced antibacterial activity of 51 was mirrored by more potent gyrase inhibition as compared with that of 50 (IC$_{50}$ = 0.59 and 3.7 μM, respectively). Although compound 50 showed essentially no hERG inhibition (IC$_{50}$ > 100 μM), compound 51 was a surprisingly potent inhibitor, with an IC$_{50}$ of 3.2 μM. The precise origin of this significantly different behavior is not understood at the present time, although it is worth noting that 51 is substantially more lipophilic than 50. Neither compound inhibited human topoisomerase IIα by >3% at 100 μM. Additional research directed at this intriguing series of amide analogues is underway and will be reported in due course.

In the third strategy, we sought to remove the secondary amine entirely, replacing it with a methylene unit. Compound 52 (Table 7) was synthesized as a roughly 3:1 mixture of cis− trans isomers (see the Supporting Information). In contrast to the analogous amine derivative (3, Table 1), 52 was wholly devoid of antibacterial activity. Consequently, it was neither separated nor assayed for hERG inhibition. These results are consistent with the accepted NBTI binding mode with S. aureus DNA gyrase, in which an amine or secondary amide interacts with aspartate 83.[13,26,27]

CONCLUSION

In summary, we have synthesized and further investigated a diverse series of dioxane-linked NBTIs using a variety of biochemical, microbiological, and safety assays. Future studies will be necessary to characterize other important druglike properties such as metabolic stability. Secondary amine derivatives bearing a monocyclic enzyme-binding moiety with a lipophilic para substituent possessed potent antistaphylococcal activity. Incorporation of a fluorinated naphthyridine DNA-binding motif robustly enhanced the antibacterial activity and TopoIV inhibition of compounds 37−41 with minimal impact on the hERG profile. In contrast, quinoxalinone and isoxazoloquinolinone derivatives did not positively differentiate from the quinoline series. It was found that hERG inhibition could be substantially reduced without loss of antibacterial activity in amide analogue 50. Dioxane-linked NBTIs thus offer promise for further optimization into novel therapeutics for treating antibiotic-resistant infections.

EXPERIMENTAL SECTION

General Chemistry Information. Moisture- or air-sensitive reactions were conducted in oven-dried glassware under an atmosphere of nitrogen or argon unless otherwise noted. Dichloromethane (DCM), toluene, tetrahydrofuran (THF), and N,N-dimethylformamide (DMF) were dried before use by passage through activated alumina under nitrogen. Flash chromatography was performed using a Teledyne-ISCO Combiflash-Rf$^+$.

^{1}H NMR spectra were recorded at either 300 or 400 MHz using residual protiated solvent as the internal reference: CDCl$_3$ (7.26 ppm), CD$_3$OD (3.31), or DMSO-d_6 (2.50 ppm). Assayed compounds had a purity of >90% as determined by ^{1}H NMR analysis. ^{13}C NMR spectra were recorded at 75 or 100 MHz using the solvent signal as the internal reference: CDCl$_3$ (77.16 ppm), CD$_3$OD (49.00), or DMSO-d_6 (39.52 ppm). High-resolution mass spectrometry was performed using electrospray ionization. The equatorial protons at C$_4$ and C$_6$ of the trans-dioxane ring typically appear as an apparent doublet of doublets at ca. 4.1−4.2 ppm in the analogues described below.[53] Careful inspection in some cases reveals additional partially resolved splitting, arising from W-coupling of these magnetically nonequivalent protons as well as virtual coupling. The additional splitting can be effectively replicated using computer simulation of nonfirst-order effects[54] with a W-coupling constant of 1.8 Hz. For the sake of clarity and consistency, this peak is labeled a doublet of doublets in the characterization data provided below.

Synthesis and Characterization of Compounds 37−42. The synthesis of compounds 37−42 is shown in Scheme 1.

8-Bromo-7-fluoro-2-methoxy-1,5-naphthyridine (33). Into a solution of commercial 3-fluoro-6-methoxy-1,5-naphthyridin-4-ol (32, 0.8625 g, 4.442 mmol, 1.0 equiv) in DMF (10 mL) was dropped phosphorus tribromide (466 μL, 5.0 mmol) at 0 °C under N$_2$ atmosphere. The reaction mixture was stirred for 1 h; then water (200 mL) and aqueous sodium hydroxide solution (6 N, 740 μL) were added. The reaction mixture was stirred for 2 h, and the precipitated solid was collected by filtration to afford the title compound as a tan solid (1.03 g, 90% yield).

^{1}H NMR (300 MHz, CDCl$_3$) δ 8.62 (s, 1H); 8.21 (d, J = 9.0 Hz, 1H); 7.13 (d, J = 9.0 Hz, 1H); 4.17 (s, 3H).

2-(2-(2-(3-Fluoro-6-methoxy-1,5-naphthyridin-4-yl)ethyl)-trans-1,3-dioxan-5-yl)isoindoline-1,3-dione (35). To a solution of 2-(2-vinyl-trans-1,3-dioxan-5-yl)isoindoline-1,3-dione (34;[25] 155.6 mg, 0.6002 mmol, 1.2 equiv relative to 33) in THF (3 mL) was added dropwise 9-borabicyclo[3.3.1]nonane solution (1.2 mL, 0.5 M in THF, 0.6 mmol, 1.0 equiv relative

to **34**) at room temperature under N₂ atmosphere. The mixture was stirred for 3 h and used directly in the next step.

To a mixture of **33** (128.5 mg, 0.5000 mmol, 1.0 equiv), cesium carbonate (325.8 mg, 1.000 mmol), and [1,1′-bis(diphenylphosphino)ferrocene] dichloropalladium(II) (13.4 mg, 0.0183 mmol, 0.04 equiv) in THF (3 mL) was added dropwise the fresh solution described above at room temperature under N₂ atmosphere. The reaction mixture was stirred overnight. The solvent was then removed in vacuo, and the residue was dissolved in DCM and washed with brine. The organic layer was concentrated and purified by chromatography on silica gel with hexane/ethyl acetate (3:1) to give the title compound as a white solid (126.4 mg, 58% yield).

¹H NMR (300 MHz, CDCl₃) δ 8.61 (s, 1H); 8.16 (d, J = 9.0 Hz, 1H); 7.84–7.80 (m, 2H); 7.77–7.68 (m, 2H); 7.06 (d, J = 9.0 Hz, 1H); 4.73 (t, J = 5.0 Hz, 1H); 4.69–4.54 (m, 1H); 4.39 (t, J = 10.6 Hz, 2H); 4.11 (s, 3H); 4.02 (dd, J = 10.7, 4.8 Hz, 2H); 3.32 (t, J = 7.3 Hz, 2H); 2.13 (td, J = 7.7, 5.2 Hz, 2H).

2-(2-(3-Fluoro-6-methoxy-1,5-naphthyridin-4-yl)ethyl)-trans-1,3-dioxan-5-amine (36). A mixture of **35** (218.7 mg, 0.5000 mmol, 1.0 equiv), ethanolamine (46 µL, 7.6 mmol, 1.5 equiv), and ethyl acetate (4 mL) was stirred and heated at 70 °C overnight. The solvent was removed, and the residue was dissolved in DCM and washed with brine. The organic layer concentrated, and the crude product was purified by chromatography on silica gel with DCM/methanol (15:1) to give the title compound as an oil (123.1 mg, 80% yield).

¹H NMR (CDCl₃) δ 8.58 (s, 1H); 8.14 (d, J = 9.0 Hz, 1H); 7.03 (d, J = 9.0 Hz, 1H); 4.41 (t, J = 5.1 Hz, 1H); 4.14–4.06 (m, 5H); 3.26–3.14 (m, 4H); 3.08–3.00 (m, 1H); 2.09–1.97 (m, 2H); 1.09 (br s, 2H).

Reductive-Amination General Procedure. To a solution of amine **36** (0.2 mmol) in methanol (2 mL) was added the requisite aldehyde (0.2 mmol) and zinc chloride (2 mg, 0.015 mmol, 0.07 equiv). The mixture was stirred at room temperature for 30 min; this was followed by the addition of sodium cyanoborohydride (40 mg, 0.6 mmol, 3.0 equiv). The reaction mixture was stirred at room temperature overnight and then purified by chromatography on silica gel with DCM/methanol (50:1). On occasion, the product obtained from flash chromatography was contaminated by a BH₃ adduct, seen in the ¹H NMR spectrum as four broad peaks from 0.00 to 0.88 ppm. In these instances, the column-purified material was dissolved in methanol (2 mL) and stirred overnight at ambient temperature with Amberlite IRA743 free base (ca. 100 mg). The pure title compound was then obtained by removal of the resin by filtration and removal of the solvent under reduced pressure.

N-((2,3-Dihydrobenzo[b][1,4]dioxin-6-yl)methyl)-2-(2-(3-fluoro-6-methoxy-1,5-naphthyridin-4-yl)ethyl)-trans-1,3-di-oxan-5-amine (37). The title compound was prepared in 52% yield following the general method and obtained as a white solid. ¹H NMR (300 MHz, CDCl₃) δ 8.59 (s, 1H); 8.15 (d, J = 9.0 Hz, 1H); 7.04 (d, J = 9.0 Hz, 1H); 6.71–6.81 (m, 3H); 4.44 (t, J = 5.0 Hz, 1H); 4.23 (s, 4H); 4.15 (dd, J = 11.1, 4.7 Hz, 2H); 4.07 (s, 3H); 3.67 (s, 2H); 3.21–3.27 (m, 4H); 2.90–2.95 (m, 1H); 2.05 (td, J = 7.6, 5.2 Hz, 2H). ¹³C NMR (75 MHz, CDCl₃) δ 162.3, 158.8, 155.4, 143.5, 142.7, 141.6, 141.5, 140.1, 138.48, 138.45, 138.1, 137.7, 133.5, 131.8, 131.6, 120.9, 117.2, 116.8, 115.11, 115.07, 101.6, 71.6, 64.4, 64.3, 53.8, 50.8, 49.6, 33.5, 18.3. HRMS (ESI) *m/z* calcd for C₂₄H₂₇FN₃O₅ [M + H]⁺: 456.1934; found: 456.1910.

N-(3,4-Dichlorobenzyl)-2-(2-(3-fluoro-6-methoxy-1,5-naphthyridin-4-yl)ethyl)-trans-1,3-dioxan-5-amine (38). The title compound was prepared in 45% yield following the general method and obtained as a white solid. ¹H NMR (300 MHz, CDCl₃) δ 8.60 (s, 1H); 8.16 (d, J = 9.0 Hz, 1H); 7.37–7.42 (m, 2H); 7.13 (dd, J = 8.2, 1.8 Hz, 1H); 7.06 (d, J = 9.0 Hz, 1H); 4.45 (t, J = 5.0 Hz, 1H); 4.16 (dd, J = 11.2, 4.7 Hz, 2H); 4.08 (s, 3H); 3.76 (s, 2H) 3.24–3.35 (m, 4H); 2.88–2.95 (m, 1H); 2.07 (td, J = 7.6, 5.3 Hz, 2H). ¹³C NMR (75 MHz, CDCl₃) δ 162.3, 158.8, 155.4, 141.6, 141.5, 140.5, 140.1, 138.51, 138.48, 138.1, 137.7, 132.6, 131.7, 131.5, 131.1, 130.4, 129.8, 127.2, 115.14, 115.10, 101.6, 71.4, 53.8, 50.1, 49.9, 33.4, 18.3. HRMS (ESI) *m/z* calcd for C₂₂H₂₃Cl₂FN₃O₃ [M + H]⁺: 466.1100; found: 466.1088.

N-((3,4-Dihydro-2H-pyrano[2,3-c]pyridin-6-yl)methyl)-2-(2-(3-fluoro-6-methoxy-1,5-naphthyridin-4-yl)ethyl)-trans-1,3-dioxan-5-amine (39). The title compound was prepared in 77% yield following the general method and obtained as a thin film. ¹H NMR (300 MHz, CDCl₃) δ 8.58 (s, 1H); 8.14 (d, J = 9.0 Hz, 1H); 8.05 (s, 1H); 7.04 (d, J = 9.0 Hz, 1H); 6.95 (s, 1H); 4.47 (t, J = 5.0 Hz, 1H); 4.22–4.15 (m, 4H); 4.07 (s, 3H); 3.81 (s, 2H); 3.37 (t, J = 10.8 Hz, 2H); 3.26 (t, J = 7.6 Hz, 2H); 3.02–2.95 (m, 1H); 2.76 (t, J = 6.5 Hz, 2H); 2.08–2.00 (m, 4H). ¹³C NMR (75 MHz, CDCl₃) δ 162.3, 158.8, 155.37, 151.35, 148.9, 141.6, 141.5, 140.1, 138.48, 138.45, 138.1, 137.7, 131.7, 131.6, 122.9, 115.14, 115.10, 101.6, 70.9, 66.6, 53.8, 51.4, 50.0, 33.4, 24.3, 21.5, 18.3. HRMS (ESI) *m/z* calcd for C₂₄H₂₇FN₄NaO₄ [M + Na]⁺: 477.1914; found: 477.1895.

N-((2,3-Dihydro-[1,4]dioxino[2,3-c]pyridin-7-yl)methyl)-2-(2-(3-fluoro-6-methoxy-1,5-naphthyridin-4-yl)ethyl)-trans-1,3-dioxan-5-amine (40). The title compound was prepared in 43% yield following the general method and obtained as a thin film. ¹H NMR (300 MHz, CDCl₃) δ 8.58 (s, 1H); 8.14 (d, J = 9.0 Hz, 1H); 8.08 (s, 1H); 7.04 (d, J = 9.0 Hz, 1H); 6.75 (s, 1H); 4.44 (t, J = 5.0 Hz, 1H); 4.33–4.23 (m, 4H); 4.15 (dd, J = 11.2, 4.7 Hz, 2H); 4.06 (s, 3H); 3.75 (s, 2H); 3.35–3.22 (m, 4H); 3.00–2.86 (m, 1H); 2.04 (td, J = 7.6, 5.2 Hz, 2H). ¹³C NMR (75 MHz, CDCl₃) δ 162.3, 158.8, 155.4, 152.9, 150.2, 141.6, 141.5, 140.2, 140.1, 138.9, 138.46, 138.44, 138.1, 137.7, 131.8, 131.6, 115.12, 115.08, 110.6, 101.6, 71.5, 65.0, 64.0, 53.8, 52.0, 49.9, 33.5, 18.3. HRMS (ESI) *m/z* calcd for C₂₃H₂₆FN₄O₅ [M + H]⁺: 457.1887; found: 457.1871.

N-((6,7-Dihydro-[1,4]oxathiino[2,3-c]pyridazin-3-yl)-methyl)-2-(2-(3-fluoro-6-methoxy-1,5-naphthyridin-4-yl)-ethyl)-trans-1,3-dioxan-5-amine (41). The title compound was prepared in 58% yield following the general method and obtained as light-yellow solid. ¹H NMR (300 MHz, CDCl₃) δ 8.58 (s, 1H); 8.14 (d, J = 9.0 Hz, 1H); 7.27 (s, 1H); 7.04 (d, J = 9.0 Hz, 1H); 4.66–4.61 (m, 2H); 4.46 (t, J = 4.8 Hz, 1H); 4.20 (dd, J = 11.1, 4.7 Hz, 2H); 4.07 (s, 3H); 3.96 (s, 2H); 3.38–3.22 (m, 4H); 3.22–3.17 (m, 2H); 3.03–2.90 (m, 1H); 2.07–2.01 (m, 2H). ¹³C NMR (75 MHz, CDCl₃) δ 162.4, 160.1, 158.9, 156.0, 155.5, 141.7, 141.6, 140.2, 138.61, 138.59, 138.2, 137.8, 131.8, 131.7, 126.0, 125.2, 115.25, 115.22, 101.7, 71.2, 66.3, 53.9, 50.12, 50.09, 33.5, 25.7, 18.4. HRMS (ESI) *m/z* calcd for C₂₂H₂₅FN₅O₄S [M + H]⁺: 474.1611; found: 474.1614.

N-(3,4-Difluorobenzyl)-2-(2-(3-fluoro-6-methoxy-1,5-naphthyridin-4-yl)ethyl)-trans-1,3-dioxan-5-amine (42). The title compound was prepared in 43% yield following the general method and obtained as a white solid. ¹H NMR (400 MHz, CDCl₃) δ 8.59 (s, 1H); 8.15 (d, J = 9.0 Hz, 1H); 7.18–

7.03 (m, 3H); 7.02−6.97 (m, 1H); 4.44 (t, J = 5.1 Hz, 1H); 4.18−4.13 (m, 2H); 4.07 (s, 3H); 3.75 (s, 2H); 3.30−3.22 (m, 4H); 2.97−2.89 (m, 1H); 2.11−2.02 (m, 2H). ^{13}C NMR (100 MHz, CDCl$_3$) δ 162.3, 158.4, 155.8, 151.7, 151.5, 150.8, 150.7, 149.2, 149.1, 148.4, 148.2, 141.6, 141.5, 140.1, 138.49, 138.47, 138.0, 137.7, 137.32, 137.27, 137.2, 131.7, 131.6, 123.63, 123.60, 123.57, 123.5, 117.2, 117.0, 116.6, 115.2, 115.1, 101.6, 71.5, 53.8, 50.3, 49.8, 33.4, 18.3. HRMS (ESI) m/z calcd for C$_{22}$H$_{23}$F$_3$N$_3$O$_3$ [M + H]$^+$: 434.1691; found: 434.1682.

The synthesis and characterization of novel compounds **3−6**, **8−30**, and **43−52** are described in the Supporting Information.

Determination of Minimum Inhibitory Concentrations (MICs). MICs against the strains listed in Tables 1, 2, 5, and 7 were determined by broth microdilution according to the guidelines established by the Clinical and Laboratory Standards Institute.[34]

Studies on the Frequency of Spontaneous Resistance. In order to determine the spontaneous-mutation frequencies of investigational agents, the MICs were first determined using the agar-dilution method as recommended by the Clinical and Laboratory Standards Institute.[34,42] The test agents and ciprofloxacin were assayed using a drug-concentration range of 0.008−8 μg/mL. Triplicate independent inocula of *S. aureus* ATCC 29213 were evaluated.

Serial dilutions of the experimental compounds were made in DMSO; that of ciprofloxacin was made in water. Agar plates were prepared by mixing 1.25 mL of concentrated drug (40× the agar-dilution MIC) with 48.75 mL of molten (52 °C) Mueller−Hinton Agar and pouring the agar into 15 × 150 mm Petri dishes; the plates were then allowed to solidify and dry at room temperature prior to inoculation. Duplicate plates were prepared to contain the agents at 4× and 8× the agar-dilution MIC. In addition, single 4× MIC and 8× MIC plates (standard small Petri plates) were prepared and inoculated according to CLSI[34] for the agar-dilution assay. This was to confirm that the drug contents of the plates were above the MIC, validating that the stock solutions of drugs were made properly.

The inoculum for the assay was prepared by streaking *S. aureus* ATCC 29213 onto six TSAB plates and incubating them for approximately 20 h at 35 °C. Using a sterile swab, several well-isolated colonies were removed and resuspended in sterile saline at a heavy concentration equivalent to 1.6 on the turbidimeter. This suspension was diluted 1:10 in order to achieve a target inoculum of 10^9 CFU on each spontaneous-mutation plate. Each plate was inoculated with 0.2 mL of the cell suspension, resulting in each drug being tested at 4× and 8× the MIC in duplicate. In addition, a portion of the inoculum was enumerated by making dilutions and spreading them onto TSA, followed by counting of colonies after a 24 h incubation at 35 °C.

Once the inoculum was absorbed into the agar, the drug-containing plates were incubated at 35 °C for 48 h and the colonies were counted. The spontaneous-mutation frequency was determined by counting the number of colonies that appeared at a given drug concentration, averaging the counts from the duplicate plates, and dividing by the number of bacteria applied to the agar surface.

Topoisomerase Inhibition. The assays were conducted at Inspiralis, Ltd. (Norwich, U.K.) unless otherwise noted. Average (mean) values are reported in cases where compounds were assayed multiple times. In all experiments, the activities of the enzymes were determined prior to testing of the

compounds, and 1 U was defined as the amount of enzyme required to fully supercoil or decatenate the substrate. This amount of enzyme was initially used in determination of control-inhibitor activity. These experiments were performed in duplicate.

Stocks (10 mM in 100% DMSO) of the compounds were serially diluted to 10% DMSO at concentrations ranging from 50 nM to 1 mM. A drug dilution or DMSO (3.0 μL) was added to a final reaction mixture of 30 μL in which the final DMSO concentration was 1% in all. Bands were visualized by ethidium staining for 20 min and destaining for 20 min. Gels were scanned using documentation equipment (GeneGenius, Syngene, Cambridge, U.K.) and percent inhibition levels (where appropriate) were obtained with gel-scanning software (GeneTools, Syngene, Cambridge, U.K.).

Staphylococcus aureus Gyrase Supercoiling Assay. DNA gyrase (1 U) was incubated with 0.5 μg of relaxed pBR322 DNA in a 30 μL reaction at 37 °C for 30 min under the following conditions: 40 mM HEPES-KOH (pH 7.6), 10 mM magnesium acetate, 10 mM DTT, 2 mM ATP, 500 mM potassium glutamate, and 0.05 mg/mL BSA. Each reaction was stopped by the addition of 30 μL of chloroform/iso-amyl alcohol (26:1) and 30 μL of Stop Dye (40% sucrose, w/v; 100 mM Tris-HCl (pH 7.5); 10 mM EDTA; 0.5 μg/mL bromophenol blue) before being loaded on a 1.0% TAE gel run at 70 V for 2 h.

Staphylococcus aureus TopoIV Decatenation Assay. Decatenation assays were performed as per the protocol by Inspiralis, Ltd. (Norwich, U.K.) where indicated (Method A). Briefly, decatenation of 200 ng of kDNA was performed at 37 °C for 30 min in a total reaction volume of 30 μL containing 50 mM Tris-HCl (pH 7.5), 5 mM MgCl$_2$, 5 mM DTT, 1.5 mM ATP, 350 mM potassium glutamate, 0.05 mg/mL BSA, 1% DMSO vehicle control (or compound solution), and 1 U of TopoIV (defined as that amount of enzyme to just completely decatenate kDNA). Each reaction was stopped by the addition of 30 μL of chloroform/isoamyl alcohol (26:1) and 30 μL of a buffer containing 40% (w/v) sucrose, 100 mM Tris-HCl (pH 8), 10 mM EDTA, and 0.5 mg/mL bromophenol blue. Aqueous fractions (20 μL) were loaded onto a 1% agarose gel, run at 70 V for 2 h, and stained with ethidium bromide for subsequent UV visualization and quantitation of the percent decatenation in the presence or absence of various concentrations of test compounds for the assessment of 50% inhibitory concentrations. Where noted, results were obtained at The Ohio State University based on slight modifications (Method B), in which reactions contained 100 ng kDNA, were incubated for 20 min, and contained final DMSO concentrations of 1.7% in the reaction mixtures.

Human Topoisomerase IIα Decatenation Assay. Human topo II (1 U) was incubated with 200 ng of kDNA in a 30 μL reaction at 37 °C for 30 min under the following conditions: 50 mM Tris-HCl (pH 7.5), 125 mM NaCl, 10 mM MgCl$_2$, 5 mM DTT, 0.5 mM EDTA, 0.1 mg/mL bovine-serum albumin (BSA), and 1 mM ATP. Each reaction was stopped by the addition of 30 μL of chloroform/iso-amyl alcohol (26:1) and 30 μL of Stop Dye before being loaded on a 1.0% TAE gel run at 90 V for 2 h.

Growth Inhibition. Log-phase parental K562 and cloned K/VP.5 cells were adjusted to 1 × 10^5 and 1.25 × 10^5 cell/mL respectively, and incubated for 48 h with 0−200 μM NBTIs, after which cells were counted on a model ZBF Coulter counter (Beckman Coulter, Danvers, MA). Growth beyond the

Table 8. Primers Used in DNA Amplification

gene	sense (5′) primer	antisense (3′) primer
gyrA_A	5′-ACTCTTGATGGCTGAATTACCTC-3′	5′-CCGCTATACCTGATGCTCCA-3′
gyrA_B	5′-GGAGCATCAGGTATAGCGGTAG-3′	5′-GGTCTACCATTTACAAGTGCAATC-3′
gyrA_C	5′-TGATTGCACTTGTAAATGGTAGAC-3′	5′-CACCACGGTTTTGAGCACG-3′
gyrA_D	5′-ATATCGTGCTCAAAACCGTGG-3′	5′-AGCCCTACAACTTCGTCACC-3′
gyrA_E	5′-GGTGACGAAGTTGTAGGGCT-3′	5′-TCTAGCATAAAAATAAGACTCCCCT-3′

starting concentrations in drug-treated versus control cells was ultimately expressed as percent inhibition of control growth. The 50% growth-inhibitory concentration for each NBTI in each cell line was calculated from concentration−response curves generated by use of Sigmaplot 13 (Systat Software, Inc., San Jose, CA). All NBTI were dissolved in 100% DMSO and added to cell suspensions to achieve a final solvent concentration of 0.5%.

hERG Inhibition. Assays were conducted at Charles River (Cleveland, OH) using IonWorks Barracuda systems (Molecular Devices Corporation, Union City, CA). Evaluations were conducted using four replicates per concentration for each compound. Cisapride was employed as the positive control.

TopoIV-Homology Model and Ligand-Placement Methods. To find usable homologues for *S. aureus* TopoIV, the protein databank was searched using BLAST.[55] Templates were selected with the following criteria: they had to be ABAB heterotetramers and DNA-bound, and there had to be high homology in both A and B. Rather than modeling the entire sequence, we chose to only model the following portions of chain A and B (which contained both the DNA- and ligand-binding sites), respectively: 5−486 and 410−637. From this, the following four homologues were selected with high percent identity/similarity with respect to *S. aureus* TopoIV in chains A and B, respectively: 4Z2C (48.6/70.3, 41.2/57.7), 5IWI (47.9/70.7, 46.3/63.0), 5CDN (48.0/70.6, 45.7/62.1), and 3FOE (56.4/74.1, 67.8/77.0). From these homologues, by assigning equal weights for each homologue, RosettaCM[56] was used to build 5000 models of the protein complex without DNA bound. These 5000 models were clustered using Rosetta with a cluster radius of 7.5 Å. The top cluster contained 94% of the structures, including the top-scoring model. This cluster center was symmetrized and relaxed in Rosetta. Next, DNA from 2XCS (*S. aureus* gyrase) was aligned into the DNA-binding pocket, and the enzyme was subsequently relaxed with respect to the DNA. To determine a potential binding conformation for compound **37**, we first built the 3D coordinates using Maestro.[57] Finally, the ligand was placed in the binding pocket and relaxed in Rosetta.

DNA Sequencing. *S. aureus* ATCC 29213 and USA 300 were grown in BBL Mueller−Hinton II Broth cation-adjusted (BD, catalogue no. 212322) medium for ∼16 h in a shaking 37 °C incubator. Genomic DNA was then isolated using protocols from the Qiagen DNeasy Blood & Tissue Handbook (Qiagen, catalogue no. 69506).

Amplification of gyrA. For amplification of the *gyrA* genes of these strains, a series of primers were designed to amplify ∼500 bp at a time (see Table 8). Briefly, purified genomic DNA was mixed with both forward and reverse primers along with Q5 High Fidelity 2× Master Mix (NEB, catalogue no. M0492S/L) and water according to the manufacturer's recommended protocol. PCR was performed in a MyCycler thermal cycler from Biorad using the following conditions: 30 cycles of 1 min at 90 °C for denaturation, 1 min at 65 °C for

annealing, and 30 s at 72 °C for polymerization. Fragments were then run on 1% agarose gels for size verification and purified using a QIAquick PCR Purification Kit (Qiagen, catalogue no. 28106).

DNA Sequencing and Analysis. Sequencing was completed by the Sanger method, and analysis was carried out using MacVector version 17 software. Multiple alignments were performed using the CLUSTAL multiple-alignment method. Two amino acid substitutions were identified in GyrA of USA 300 relative to the ATCC strain: S84L and T457A. S84L is commonly encountered in fluoroquinolone-resistant *S. aureus* isolates.[58] Variability in position 457 (A vs T) has been reported in fluoroquinolone-susceptible strains and is thus not likely connected to resistance.[58]

■ ASSOCIATED CONTENT

Ⓢ Supporting Information

The Supporting Information is available free of charge on the ACS Publications website at DOI: 10.1021/acsinfec-dis.8b00375.

> Experimental details on the synthesis and characterization of compounds **3−6**, **8−31**, and **43−52** (PDF)

■ AUTHOR INFORMATION

Corresponding Author

*E-mail: mitton-fry.1@osu.edu. Tel.: +1-614-292-1903.

ORCID Ⓞ

Steffen Lindert: 0000-0002-3976-3473

Mark J. Mitton-Fry: 0000-0002-6715-8836

Notes

■ ACKNOWLEDGMENTS

Karl Werbovetz and James Fuchs (The Ohio State University) for helpful discussions.

■ REFERENCES

(1) Tacconelli, E., Carrara, E., Savoldi, A., Harbarth, S., Mendelson, M., Monnet, D. L., Pulcini, C., Kahlmeter, G., Kluytmans, J., Carmeli, Y., Ouellette, M., Outterson, K., Patel, J., Cavaleri, M., Cox, E. M., Houchens, C. R., Grayson, M. L., Hansen, P., Singh, N., Theuretzbacher, U., and Magrini, N. (2018) Discovery, Research, and Development of New Antibiotics: the WHO Priority List of Antibiotic-resistant Bacteria and Tuberculosis. *Lancet Infect. Dis.* 18, 318−327.

(2) Tong, S. Y. C., Davis, J. S., Eichenberger, E., Holland, T. L., and Fowler, V. G. (2015) *Staphylococcus aureus* Infections: Epidemiology, Pathophysiology, Clinical Manifestations, and Management. *Clin. Microbiol. Rev.* 28, 603−661.

(3) Goss, C. H., and Muhlebach, M. S. (2011) Review: *Staphylococcus aureus* and MRSA in Cystic Fibrosis. *J. Cystic Fibrosis* 10, 298−306.

(4) CDC (2013) *Antibiotic Resistance Threats in the United States, 2013*, U.S. Centers for Disease Control and Prevention, https://www.cdc.gov/drugresistance/threat-report-2013/index.html (accessed Dec 3, 2018).

(5) Rodvold, K. A., and McConeghy, K. W. (2014) Methicillin-Resistant *Staphylococcus aureus* Therapy: Past, Present, and Future. *Clin. Infect. Dis.* 58 (S1), S20−S27.

(6) David, M. Z., Dryden, M., Gottlieb, T., Tattevin, P., and Gould, I. M. (2017) Recently Approved Antibacterials for Methicillin-Resistant *Staphylococcus aureus* (MRSA) and other Gram-Positive Pathogens: The Shock of the New. *Int. J. Antimicrob. Agents* 50, 303−307.

(7) Markham, A. (2017) Delafloxacin: First Global Approval. *Drugs* 77, 1481−1486.

(8) Markham, A., and Keam, S. J. (2018) Omadacycline: First Global Approval. *Drugs* 78, 1931−1937.

(9) Zhanel, G. G., Cheung, D., Adam, H., Zelenitsky, S., Golden, A., Schweizer, F., Gorityala, B., Lagacé-Wiens, P. R. S., Walkty, A., Gin, A. S., Hoban, D. J., and Karlowsky, J. A. (2016) Review of Eravacycline, a Novel Fluorocycline Antibacterial Agent. *Drugs* 76, 567−588.

(10) Lee, H., Yoon, E.-J., Kim, D., Kim, J. W., Lee, K.-J., Kim, H. S., Kim, Y. R., Shin, J. H., Shin, J. H., Shin, K. S., Kim, Y. A., Uh, Y., and Jeong, S. H. (2018) Ceftaroline Resistance by Clone-Specific Polymorphism in Penicillin-Binding Protein 2a of Methicillin-Resistant *Staphylococcus aureus*. *Antimicrob. Agents Chemother.* 62, e00485−18.

(11) Mitton-Fry, M. J. (2017) Novel Bacterial Type II Topoisomerase Inhibitors. *Med. Chem. Rev.* 52, 281−302.

(12) Mayer, C., and Janin, Y. L. (2014) Non-Quinolone Inhibitors of Bacterial Type IIA Topoisomerases: A Feat of Bioisosterism. *Chem. Rev.* 114, 2313−2342.

(13) Bax, B. D., Chan, P. F., Eggleston, D. S., Fosberry, A., Gentry, D. R., Gorrec, F., Giordano, I., Hann, M. M., Hennessy, A., Hibbs, M., Huang, J., Jones, E., Jones, J., Brown, K. K., Lewis, C. J., May, E. W., Saunders, M. R., Singh, O., Spitzfaden, C. E., Shen, C., Shillings, A., Theobald, A. J., Wohlkonig, A., Pearson, N. D., and Gwynn, M. N. (2010) Type IIα Topoisomerase Inhibition by a New Class of Antibacterial Agents. *Nature* 466, 935−940.

(14) Gibson, E. G., Bax, B., Chan, P. F., and Osheroff, N. (2019) Mechanistic and Structural Basis for the Actions of the Antibacterial Gepotidacin against *Staphylococcus aureus* Gyrase. *ACS Infect. Dis.* 5 (4), 570−581.

(15) O'Riordan, W., Tiffany, C., Scangarella-Oman, N., Perry, C., Hossain, M., Ashton, T., and Dumont, E. (2017) Efficacy, Safety, and Tolerability of Gepotidacin (GSK2140944) in the Treatment of Patients with Suspected or Confirmed Gram-Positive Acute Bacterial Skin and Skin Structure Infections. *Antimicrob. Agents Chemother.* 61, e02095−16.

(16) Taylor, S. N., Morris, D. H., Avery, A. K., Workowski, K. A., Batteiger, B. E., Tiffany, C. A., Perry, C. R., Raychaudhuri, A., Scangarella-Oman, N. E., Hossain, M., and Dumont, E. F. (2018) Gepotidacin for the Treatment of Uncomplicated Urogenital Gonorrhea: A Phase 2, Randomized, Dose-Ranging, Single-Oral Dose Evaluation. *Clin. Infect. Dis.* 67, 504−512.

(17) Kolarič, A., and Minovski, N. (2018) Novel Bacterial Topoisomerase Inhibitors: Challenges and Perspectives in Reducing hERG Toxicity. *Future Med. Chem.* 10, 2241−2244.

(18) Hossain, M., Zhou, M., Tiffany, C., Dumont, E., and Darpo, B. (2017) A Phase I, Randomized, Double-Blinded, Placebo- and Moxifloxacin-Controlled Four-Period Crossover Study to Evaluate the Effect of Gepotidacin on Cardiac Conduction as Assessed by 12-Lead Electrocardiogram Conduction in Healthy Volunteers. *Antimicrob. Agents Chemother.* 61, e02385−16.

(19) Black, M. T., and Coleman, K. (2009) New Inhibitors of Bacterial Topoisomerase GyrA/ParC Subunits. *Curr. Opin. Invest. Drugs* 10, 804−810.

(20) Reck, F., Alm, R. A., Brassil, P., Newman, J. V., Ciaccio, P., McNulty, J., Barthlow, H., Goteti, K., Breen, J., Comita-Prevoir, J., Cronin, M., Ehmann, D. E., Geng, B., Godfrey, A. A., and Fisher, S. L. (2012) Novel N-Linked Aminopiperidine Inhibitors of Bacterial Topoisomerase Type II with Reduced pKₐ: Antibacterial Agents with an Improved Safety Profile. *J. Med. Chem.* 55, 6916−6933.

(21) Black, M. T., Stachyra, T., Platel, D., Girard, A.-M., Claudon, M., Bruneau, J.-M., and Miossec, C. (2008) Mechanism of Action of the Antibiotic NXL101, a Novel Nonfluoroquinolone Inhibitor of Bacterial Type II Topoisomerases. *Antimicrob. Agents Chemother.* 52, 3339−3349.

(22) Mitton-Fry, M. J., Brickner, S. J., Hamel, J. C., Brennan, L., Casavant, J. M., Chen, M., Chen, T., Ding, X., Driscoll, J., Hardink, J., Hoang, T., Hua, E., Huband, M. D., Maloney, M., Marfat, A., McCurdy, S. P., McLeod, D., Plotkin, M., Reilly, U., Robinson, S., Schafer, J., Shepard, R. M., Smith, J. F., Stone, G. G., Subramanyam, C., Yoon, K., Yuan, W., Zaniewski, R. P., and Zook, C. (2013) Novel Quinoline Derivatives as Inhibitors of Bacterial DNA Gyrase and Topoisomerase IV. *Bioorg. Med. Chem. Lett.* 23, 2955−2961.

(23) Surivet, J.-P., Zumbrunn, C., Rueedi, G., Hubschwerlen, C., Bur, D., Bruyére, T., Locher, H., Ritz, D., Keck, W., Seiler, P., Kohl, C., Gauvin, J.-C., Mirre, A., Kaegi, V., Dos Santos, M., Gaertner, M., Delers, J., Enderlin-Paput, M., and Boehme, M. (2013) Design, Synthesis, and Characterization of Novel Tetrahydropyran-Based Bacterial Topoisomerase Inhibitors with Potent Anti-Gram-Positive Activity. *J. Med. Chem.* 56, 7396−7415.

(24) Lahiri, S. D., Kutschke, A., McCormack, K., and Alm, R. A. (2015) Insights Into the Mechanism of Inhibition of Novel Bacterial Topoisomerase Inhibitors from Characterization of Resistant Mutants of *Staphylococcus aureus*. *Antimicrob. Agents Chemother.* 59, 5278−5287.

(25) Li, L., Okumu, A., Dellos-Nolan, S., Li, Z., Karmahapatra, S., English, A., Yalowich, J. C., Wozniak, D. J., and Mitton-Fry, M. J. (2018) Synthesis and Anti-Staphylococcal activity of Novel Bacterial

Topoisomerase Inhibitors with a 5-Amino-1,3-Dioxane Linker Moiety. *Bioorg. Med. Chem. Lett.* 28, 2477–2480.

(26) Singh, S. B., Kaelin, D. E., Wu, J., Miesel, L., Tan, C. M., Meinke, P. T., Olsen, D., Lagrutta, A., Bradley, P., Lu, J., Patel, S., Rickert, K. W., Smith, R. F., Soisson, S., Wei, C., Fukuda, H., Kishii, R., Takei, M., and Fukuda, Y. (2014) Oxabicyclooctane-Linked Novel Bacterial Topoisomerase Inhibitors as Broad Spectrum Antibacterial Agents. *ACS Med. Chem. Lett.* 5, 609–614.

(27) Widdowson, K., and Hennessy, A. (2010) Advances in Structure-Based Drug Design of Novel Bacterial Topoisomerase Inhibitors. *Future Med. Chem.* 2, 1619–1622.

(28) Hameed P, S., Patil, V., Solapure, S. M., Sharma, U., Madhavapeddi, P., Raichurkar, A., Chinnapattu, M., Manjrekar, P., Shanbhag, G., Puttur, J., Shinde, V., Menasinakai, S., Rudrapatana, S., Achar, V., Awasthy, D., Nandishaiah, R., Humnabadkar, V., Ghosh, A., Narayan, C., Ramya, V. K., Kaur, P., Sharma, S., Werngren, J., Hoffner, H., Panduga, V., Kumar, C. N. N., Reddy, J., Kumar KN, M., Ganguly, S., Bharath, S., Bheemarao, U., Mukherjee, K., Arora, U., Gaonkar, S., Coulson, M., Waterson, D., Sambandamurthy, V. K., and de Sousa, S. M. (2014) Novel N-Linked Aminopiperidine-Based Gyrase Inhibitors with Improved hERG and In Vivo Efficacy against *Mycobacterium tuberculosis*. *J. Med. Chem.* 57, 4889–4905.

(29) Bobesh, K. A., Renuka, J., Jeankumar, V. U., Shruti, S. K., Sridevi, J. P., Yogeeswari, P., and Sriram, D. (2014) Extending the N-Linked Aminopiperidine Class to the Mycobacterial Gyrase Domain: Pharmacophore Mapping from Known Antibacterial Leads. *Eur. J. Med. Chem.* 85, 593–604.

(30) Blanco, D., Perez-Herran, E., Cacho, M., Ballell, L., Castro, J., González del Rio, R., Lavandera, J. L., Remuiñán, M. J., Richards, C., Rullas, J., Vázquez-Muñiz, M. J., Woldu, E., Zapatero-González, M. C., Angulo-Barturen, I., Mendoza, A., and Barros, D. (2015) *Mycobacterium tuberculosis* Gyrase Inhibitors as a New Class of Antitubercular Drugs. *Antimicrob. Agents Chemother.* 59, 1868–1875.

(31) Gibson, E. G., Blower, T. R., Cacho, M., Bax, B., Berger, J. M., and Osheroff, N. (2018) Mechanism of Action of *Mycobacterium tuberculosis* Gyrase Inhibitors: A Novel Class of Gyrase Poisons. *ACS Infect. Dis.* 4, 1211–1222.

(32) Mitton-Fry, M. J., Brickner, S. J., Hamel, J. C., Barham, R., Brennan, L., Casavant, J. M., Ding, X., Finegan, S., Hardink, J., Hoang, T., Huband, M. D., Maloney, M., Marfat, A., McCurdy, S. P., McLeod, D., Subramanyam, C., Plotkin, M., Reilly, U., Schafer, J., Stone, G. G., Uccello, D. P., Wisialowski, T., Yoon, K., Zaniewski, R., and Zook, C. (2017) Novel 3-Fluoro-6-methoxyquinoline Derivatives as Inhibitors of Bacterial DNA Gyrase and Topoisomerase IV. *Bioorg. Med. Chem. Lett.* 27, 3353–3358.

(33) Griffen, E., Leach, A. G., Robb, G. R., and Warner, D. J. (2011) Matched Molecular Pairs as a Medicinal Chemistry Tool. *J. Med. Chem.* 54, 7739–7750.

(34) (2018) *Methods for Dilution Antimicrobial Susceptibility Tests for Bacteria That Grow Aerobically* 11th ed., CLSI document M07-Ed11, Clinical and Laboratory Standards Institute, Wayne, PA.

(35) Wiener, J. J. M., Gomez, L., Venkatesan, H., Santillán, A., Allison, B. D., Schwarz, K. L., Shinde, S., Tang, L., Hack, M. D., Morrow, B. J., Motley, S. T., Goldschmidt, R. M., Shaw, K. J., Jones, T. K., and Grice, C. A. (2007) Tetrahydroindazole Inhibitors of Bacterial Type II Topoisomerases. Part 2: SAR Development and Potency Against Multidrug-Resistant Strains. *Bioorg. Med. Chem. Lett.* 17, 2718–2722.

(36) Miles, T. J., Hennessy, A. J., Bax, B., Brooks, G., Brown, B. S., Brown, P., Cailleau, N., Chen, D., Dabbs, S., Davies, D. T., Esken, J. M., Giordano, I., Hoover, J. L., Huang, J., Jones, G. E., Kusalakumari Sukmar, S. K., Spitzfaden, C., Markwell, R. E., Minthorn, E. A., Rittenhouse, S., Gwynn, M. N., and Pearson, N. D. (2013) Novel Hydroxyl Tricyclics (e.g., GSK966587) as Potent Inhibitors of Bacterial Type IIA Topoisomerases. *Bioorg. Med. Chem. Lett.* 23, 5437–5441.

(37) Miles, T. J., Hennessy, A. J., Bax, B., Brooks, G., Brown, B. S., Brown, P., Cailleau, N., Chen, D., Dabbs, S., Davies, D. T., Esken, J. M., Giordano, I., Hoover, J. L., Jones, G. E., Kusalakumari Sukmar, S.

K., Markwell, R. E., Minthorn, E. A., Rittenhouse, S., Gwynn, M. N., and Pearson, N. D. (2016) Novel Tricyclics (e.g. GSK945237) as Potent Inhibitors of Bacterial Type IIA Topoisomerases. *Bioorg. Med. Chem. Lett.* 26, 2464–2469.

(38) Miles, T. J., Axten, J. M., Barfoot, C., Brooks, G., Brown, P., Chen, D., Dabbs, S., Davies, D. T., Downie, D. L., Eyrisch, S., Gallagher, T., Giordano, I., Gwynn, M. N., Hennessy, A., Hoover, J., Huang, J., Jones, G., Markwell, R., Miller, W. H., Minthorn, E. A., Rittenhouse, S., Seefeld, M., and Pearson, N. (2011) Novel Aminopiperidines as Potent Antibacterials Targeting Bacterial Type IIA Topoisomerases. *Bioorg. Med. Chem. Lett.* 21, 7489–7495.

(39) Surivet, J.-P., Zumbrunn, C., Rueedi, G., Bur, D., Bruyére, T., Locher, H., Ritz, D., Seiler, P., Kohl, C., Ertel, E. A., Hess, P., Gauvin, J.-C., Mirre, A., Kaegi, V., Dos Santos, M., Kraemer, S., Gaertner, M., Delers, J., Enderlin-Paput, M., Weiss, M., Sube, R., Hadana, H., Keck, W., and Hubschwerlen, C. (2015) Novel Tetrahydropyran-Based Bacterial Topoisomerase Inhibitors with Potent Anti-Gram Positive Activity and Improved Safety Profile. *J. Med. Chem.* 58, 927–942.

(40) Lall, M. S., Tao, Y., Arcari, J. T., Boyles, D., Brown, M. F., Damon, D. B., Lilley, S. C., Mitton-Fry, M. J., Starr, J. T., Stewart, A. M., and Sun, J. (2018) Process Development for the Synthesis of the Monocyclic β-Lactam Core 17. *Org. Process Res. Dev.* 22, 212–218.

(41) Tan, C. M., Gill, C. J., Wu, J., Toussaint, N., Yin, J., Tsuchiya, T., Garlisi, C. G., Kaelin, D., Meinke, P. T., Miesel, L., Olsen, D. B., Lagrutta, A., Fukuda, H., Kishii, R., Takei, M., Oohata, K., Takeuchi, T., Shibue, T., Takano, H., Nishimura, A., Fukuda, Y., and Singh, S. B. (2016) *In Vitro* and *In Vivo* Characterization of the Novel Oxabicyclooctane-Linked Bacterial Topoisomerase Inhibitor AM-8722, a Selective, Potent Inhibitor of Bacterial DNA Gyrase. *Antimicrob. Agents Chemother.* 60, 4830–4839.

(42) (2018) *Performance Standards for Antimicrobial Susceptibility Testing; Twenty-Eighth Informational Supplement*, CLSI document M100-S28, Clinical and Laboratory Standards Institute, Wayne, PA.

(43) Reck, F., Ehmann, D. E., Dougherty, T. J., Newman, J. V., Hopkins, S., Stone, G., Agrawal, N., Ciaccio, P., McNulty, J., Barthlow, H., O'Donnell, J., Goteti, K., Breen, J., Comita-Prevoir, J., Cornebise, M., Cronin, M., Eyermann, C. J., Geng, B., Carr, G. R., Pandarinathan, L., Tang, X., Cottone, A., Zhao, L., and Bezdenejnih-Snyder, N. (2014) Optimization of Physicochemical Properties and Safety Profile of Novel Bacterial Topoisomerase Type II Inhibitors (NBTIs) with Activity Against *Pseudomonas aeruginosa*. *Bioorg. Med. Chem.* 22, 5392–5409.

(44) Surivet, J.-P., Zumbrunn, C., Bruyére, T., Bur, D., Kohl, C., Locher, H. H., Seiler, P., Ertel, E. A., Hess, P., Enderlin-Paput, M., Enderlin-Paput, S., Gauvin, J.-C., Mirre, A., Hubschwerlen, C., Ritz, D., and Rueedi, G. (2017) Synthesis and Characterization of Tetrahydropyran-Based Bacterial Topoisomerase Inhibitors with Antibacterial Activity against Gram-Negative Bacteria. *J. Med. Chem.* 60, 3776–3794.

(45) Ritke, M. K., Roberts, D., Allan, W. P., Raymond, J., Bergoltz, V. V., and Yalowich, J. C. (1994) Altered Stability of Etoposide-Induced Topoisomerase II-DNA Complexes in Resistant Human Leukaemia K562 Cells. *Br. J. Cancer* 69, 687–697.

(46) Kanagasabai, R., Serdar, L., Karmahapatra, S., Kientz, C. A., Ellis, J., Ritke, M. K., Elton, T. S., and Yalowich, J. C. (2017) Alternative RNA Processing of Topoisomerase IIα in Etoposide-Resistant Human Leukemia K562 Cells: Intron Retention Results in a Novel C-Terminal Truncated 90-kDa Isoform. *J. Pharmacol. Exp. Ther.* 360, 152–163.

(47) Ndubaku, C. O., Crawford, J. J., Drobnick, J., Aliagas, I., Campbell, D., Dong, P., Dornan, L. M., Duron, S., Epler, J., Gazzard, L., Heise, C. E., Hoeflich, K. P., Jakubiak, D., La, H., Lee, W., Lin, B., Lyssikatos, J. P., Maksimoska, J., Marmorstein, R., Murray, L. J., O'Brien, T., Oh, A., Ramaswamy, S., Wang, W., Zhao, X., Zhong, Y., Blackwood, E., and Rudolph, J. (2015) Design of Selective PAK1 Inhibitor G-5555: Improving Properties by Employing an Unorthodox Low pK_a Polar Moiety. *ACS Med. Chem. Lett.* 6, 1241–1246.

(48) Reck, F., Alm, R., Brassil, P., Newman, J., DeJonge, B., Eyermann, C. J., Breault, G., Breen, J., Comita-Prevoir, J., Cronin, M.,

Davis, H., Ehmann, D., Galullo, V., Geng, B., Grebe, T., Morningstar, M., Walker, P., Hayter, B., and Fisher, S. (2011) Novel N-Linked Aminopiperidine Inhibitors of Bacterial Topoisomerase Type II: Broad-Spectrum Antibacterial Agents with Reduced hERG Activity. *J. Med. Chem.* 54, 7834−7847.

(49) Charrier, C., Salisbury, A.-M., Savage, V. J., Duffy, T., Moyo, E., Chaffer-Malam, N., Ooi, N., Newman, R., Cheung, J., Metzger, R., McGarry, D., Pichowicz, M., Sigerson, R., Cooper, I. R., Nelson, G., Butler, H. S., Craighead, M., Ratcliffe, A. J., Best, S. A., and Stokes, N. R. (2017) Novel Bacterial Topoisomerase Inhibitors with Potent Broad-Spectrum Activity against Drug-Resistant Bacteria. *Antimicrob. Agents Chemother.* 61, e02100−16.

(50) Gomez, L., Hack, M. D., Wu, J., Wiener, J. J. M., Venkatesan, H., Santillán, A., Pippel, D. J., Mani, N., Morrow, B. J., Motley, S. T., Shaw, K. J., Wolin, R., Grice, C. A., and Jones, T. K. (2007) Novel Pyrazole Derivatives as Potent Inhibitors of Type II Topoisomerases. Part 1. Synthesis and Preliminary SAR Analysis. *Bioorg. Med. Chem. Lett.* 17, 2723−2727.

(51) Singh, S. B., Kaelin, D. E., Wu, J., Miesel, L., Tan, C. M., Gill, C., Black, T., Nargund, R., Meinke, P. T., Olsen, D. B., Lagrutta, A., Wei, C., Peng, X., Wang, X., Fukuda, H., Kishii, R., Takei, M., Takeuchi, T., Shibue, T., Ohata, K., Takano, H., Ban, S., Nishimura, A., and Fukuda, Y. (2015) Hydroxy Tricyclic 1,5-Naphthyridinone Oxabicyclooctane-Linked Novel Bacterial Topoisomerase Inhibitors as Broad-Spectrum Antibacterial Agents-SAR of RHS Moiety (Part-3). *Bioorg. Med. Chem. Lett.* 25, 2473−2478.

(52) Davies, D. T., Jones, G. E., Markwell, R. E., Miller, W., and Pearson, N. D. (July 25, 2002) International Patent Application WO 2002/046882A1.

(53) The identified splitting pattern is characteristic for the *trans*-substituted dioxane diastereomer and notably distinct from the *cis* isomer. For earlier work, see Bailey, W. F., Lambert, K. M., Stempel, Z. D., Wiberg, K. B., and Mercado, B. O. (2016) Controlling the Conformational Energy of a Phenyl Group by Tuning the Strength of a Nonclassical CH-O Hydrogen Bond: The Case of 5-Phenyl-1,3-dioxane. *J. Org. Chem.* 81, 12116−12127.

(54) (a) Binev, Y., Marques, M. M. B., and Aires-de-Sousa, J. (2007) Prediction of ^{1}H NMR Coupling Constants with Associative Neural Networks Trained for Chemical Shifts. *J. Chem. Inf. Model.* 47, 2089−2097. (b) Online simulation conducted at www.nmrdb.org.

(55) Boratyn, G. M., Schäffer, A. A., Agarwala, R., Altschul, S. F., Lipman, D. J., and Madden, T. L. (2012) Domain Enhanced Lookup Time Accelerated BLAST. *Biol. Direct* 7, 12−25.

(56) Song, Y., DiMaio, F., Wang, R. Y.-R., Kim, D., Miles, C., Brunette, T. J., Thompson, J., and Baker, D. (2013) High-Resolution Comparative Modeling with RosettaCM. *Structure* 21, 1735−1742.

(57) (2019) *Schrödinger Release 2019-1: Maestro*, Schrödinger, LLC, New York, NY.

(58) SanFilippo, C. M., Hesje, C. K., Haas, W., and Morris, T. W. (2011) Topoisomerase Mutations that are Associated with High-Level Resistance to Earlier Fluoroquinolones in *Staphylococcus aureus* Have Less Effect on the Antibacterial Activity of Besifloxacin. *Chemotherapy* 57, 363−371.